A benthic δ^{13}C-based proxy for atmospheric pCO_2 over the last 1.5 Myr

L. E. Lisiecki[1]

Received 12 August 2010; revised 23 September 2010; accepted 28 September 2010; published 13 November 2010.

[1] A high-resolution marine proxy for atmospheric pCO_2 is needed to clarify the phase lag between pCO_2 and marine climate proxies and to provide a record of orbital-scale pCO_2 variations before the oldest ice core measurement at 800 ka. Benthic δ^{13}C data should record deep ocean carbon storage and, thus, atmospheric pCO_2. This study finds that a modified δ^{13}C gradient between the deep Pacific and intermediate North Atlantic ($\Delta\delta^{13}C_{P-\frac{NA}{2}}$) correlates well with pCO_2. $\Delta\delta^{13}C_{P-\frac{NA}{2}}$ reproduces characteristic differences between pCO_2 and ice volume during Late Pleistocene glaciations and indicates that pCO_2 usually leads terminations by 0.2–3.7 kyr but lags by 3–10 kyr during two "failed" terminations at 535 and 745 ka. $\Delta\delta^{13}C_{P-\frac{NA}{2}}$ gradually transitions from 41- to 100-kyr cyclicity from 1.3–0.7 Ma but has no secular trend in mean or amplitude since 1.5 Ma. The minimum pCO_2 of the last 1.5 Myr is estimated to be 155 ppm at ~920 ka. **Citation:** Lisiecki, L. E. (2010), A benthic δ^{13}C-based proxy for atmospheric pCO_2 over the last 1.5 Myr, *Geophys. Res. Lett.*, *37*, L21708, doi:10.1029/2010GL045109.

1. Introduction

[2] The 800-kyr record of atmospheric carbon dioxide concentration from Antarctic ice cores [*Petit et al.*, 1999; *Monnin et al.*, 2001; *Siegenthaler et al.*, 2005; *Lüthi et al.*, 2008] correlates well with Antarctic temperature [*Jouzel et al.*, 2007] and many paleoclimate proxies from marine sediments (e.g., global ice volume [*Hansen et al.*, 2007], sea surface temperatures [*Lea*, 2004]). However, age models for these two climate archives are developed independently of one another and have relative uncertainties of 5–10 kyr before 50 ka [*Lisiecki and Raymo*, 2005; *Parrenin et al.*, 2007; *Loulergue et al.*, 2007]. Therefore, the phase of marine climate proxies relative to atmospheric pCO_2 remains uncertain, preventing reconstruction of the sequence of climate responses associated with pCO_2 change before 50 ka. A high-resolution marine proxy for pCO_2 could solve this problem and extend pCO_2 estimates beyond the oldest ice core measurement.

[3] Alkenone δ^{13}C and boron-based proxies reconstruct pCO_2 concentrations in the surface ocean, but currently these records lack orbital-scale resolution and have error bars of at least ±19 ppm [*Hönisch et al.*, 2009; *Tripati et al.*, 2009; *Pagani et al.*, 2009; *Seki et al.*, 2010]. Existing higher-resolution benthic δ^{13}C records also have the potential to record changes in atmospheric pCO_2 because glacial-interglacial changes in pCO_2 are associated with changes in the ΣCO_2 and δ^{13}C of the deep ocean [*Oppo and Fairbanks*, 1990; *Flower et al.*, 2000; *Hodell et al.*, 2003; *Köhler et al.*, 2010]. This study empirically evaluates several possible benthic δ^{13}C-based proxies and uses the one best correlated with ice core pCO_2 to evaluate the phase lag between pCO_2 and benthic δ^{18}O and to estimate pCO_2 from 1.5–0.8 Ma.

2. Background

[4] Decreased deep water ventilation and increased Southern Ocean productivity are thought to reduce glacial pCO_2 by removing carbon from the surface and sequestering it in the deep ocean [e.g., *Toggweiler*, 1999; *Brovkin et al.*, 2007; *Martínez-Garcia et al.*, 2009]. These processes also decrease the δ^{13}C value of deep waters as sinking low-δ^{13}C organic carbon remineralizes at depth and glacial overturning is decreased [*Toggweiler et al.*, 2006; *Köhler et al.*, 2010]. Reduced terrestrial carbon storage is the only glacial process for which pCO_2 and benthic δ^{13}C changes are not positively correlated, increasing atmospheric pCO_2 but decreasing mean ocean δ^{13}C [*Shackleton*, 1977; *Brovkin et al.*, 2007; *Köhler et al.*, 2010]. A carbon cycle box model that includes all of these processes predicts a strong, linear relationship (r = 0.98) between pCO_2 and deep Pacific δ^{13}C, but the observed correlation is much weaker (r = 0.5) due to low-frequency (~400-kyr) variations in δ^{13}C not observed in pCO_2 [*Köhler et al.*, 2010].

[5] The δ^{13}C gradient between deep and intermediate waters ($\Delta\delta^{13}C_{D-I}$) has also been suggested as proxy for pCO_2 because it should reflect the ΣCO_2 concentration gradient between the deep ocean and better-ventilated intermediate ocean [*Oppo and Fairbanks*, 1990; *Flower et al.*, 2000; *Hodell et al.*, 2003; *Toggweiler et al.*, 2006]. $\Delta\delta^{13}C_{D-I}$ may also remove the mean-ocean δ^{13}C signal associated with changes in terrestrial carbon storage. Previous comparisons of $\Delta\delta^{13}C_{D-I}$ and pCO_2 yielded moderate correlations but did not extend beyond 400 ka [*Oppo and Fairbanks*, 1990; *Flower et al.*, 2000; *Hodell et al.*, 2003].

3. Proxy Evaluation

[6] Here I evaluate Pacific δ^{13}C, $\Delta\delta^{13}C_{D-I}$ and the average of the two as possible proxies for pCO_2. The signal-to-noise ratio of δ^{13}C signals is enhanced by averaging data from multiple cores within the same watermass to produce δ^{13}C stacks for the deep Pacific, deep South Atlantic, and intermediate North Atlantic (Figure 1 and Table S1 of Text S1 of the auxiliary material) [*Lisiecki*, 2010].[1] The deep Pacific stack is used for the deep-intermediate gradient ($\Delta\delta^{13}C_{P-NA}$)

[1]Department of Earth Science, University of California, Santa Barbara, California, USA.

0094-8276/10/2010GL045109

[1]Auxiliary materials are available in the HTML. doi:10.1029/2010GL045109.

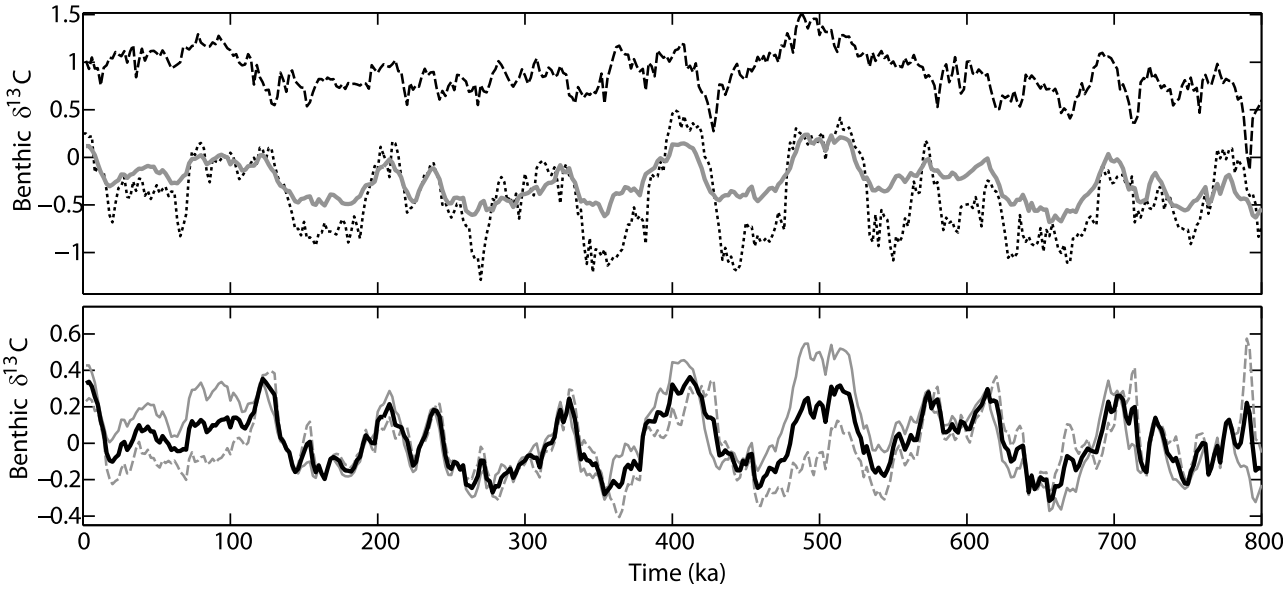

Figure 1. Benthic δ^{13}C stacks and potential pCO_2 proxies. (top) Regional stacks of benthic δ^{13}C from the intermediate North Atlantic (1145–2300 m depth, dashed line), South Atlantic (3700–4620 m, dotted), and equatorial Pacific (2520–3850 m, gray). (bottom) Pacific δ^{13}C stack (gray solid), $\Delta\delta^{13}C_{P-NA}$ (dashed), and the average of the two, $\Delta\delta^{13}C_{P-\frac{NA}{2}}$ (black solid). All three records are adjusted to have a mean of zero.

because watermass boundary movement provides an additional source of δ^{13}C variability in the deep South Atlantic [*Venz and Hodell*, 2002] that does not affect the deep Pacific [*Matsumoto et al.*, 2002; *Lisiecki*, 2010]. For further discussion see the auxiliary material. Although Pacific δ^{13}C has approximately half the glacial-interglacial amplitude of South Atlantic δ^{13}C, the following analysis is not highly sensitive to which deep water stack is used because $\Delta\delta^{13}C_{P-NA}$ and $\Delta\delta^{13}C_{SA-NA}$ are well correlated from 800–0 ka (r=0.79).

[7] Pacific δ^{13}C and $\Delta\delta^{13}C_{P-NA}$ both correlate moderately well with pCO_2, but their average $\Delta\delta^{13}C_{P-\frac{NA}{2}}$ produces the best correlation (Table 1 and Figure 1, bottom). Based on inter-core variability, $\Delta\delta^{13}C_{P-\frac{NA}{2}}$ has a 1-σ uncertainty of 0.11‰ from 0.8–0 Ma and 0.13‰ from 1.5–0.8 Ma (equivalent to 17.5 ppm and 19.2 ppm, respectively). When $\Delta\delta^{13}C_{P-\frac{NA}{2}}$ is scaled to the mean and standard deviation of ice core pCO_2, it has a root mean square error (RMSE) relative to pCO_2 of 17.5 ppm, whereas boron-based estimates have RMSE of 18.1 ppm [*Hönisch et al.*, 2009] and 24.9 ppm [*Tripati et al.*, 2009] (see auxiliary material).

[8] One possible physical explanation for the correlation between pCO_2 and $\Delta\delta^{13}C_{P-\frac{NA}{2}}$ is that δ^{13}C variability in the deep and intermediate Atlantic may be amplified relative to their Pacific and global mean counterparts, e.g., due to changes in temperature and/or deepwater formation processes in the Atlantic. Thus, $\Delta\delta^{13}C_{P-\frac{NA}{2}}$ corrects for differences in the amplitudes of variability between the Atlantic and Pacific. Alternatively, if Pacific δ^{13}C and $\Delta\delta^{13}C_{P-NA}$ are influenced differently by additional climatic processes, the average of the two should amplify the pCO_2 signal common to both.

[9] The correlation between marine proxies and pCO_2 is not a perfect evaluation metric because it depends on the particular marine and ice core chronologies used; therefore, $\Delta\delta^{13}C_{P-\frac{NA}{2}}$ is also evaluated by whether it replicates features of the pCO_2 record that are independent of age model. Here I focus on features that differ from the benthic δ^{18}O record [*Lisiecki and Raymo*, 2005] of deep water temperature and global ice volume. pCO_2 and northern hemisphere ice volume changes may differ if pCO_2 is controlled by southern hemisphere processes that are only weakly coupled to northern hemisphere climate [*Toggweiler*, 2008].

[10] One notable difference between δ^{18}O and pCO_2 (Figure 2, top) is that pCO_2 generally reaches its minimum early in each glaciation and then remains constant (e.g., Marine Isotope Stage (MIS) 6 and 12) or increases slightly (e.g., MIS 16) whereas benthic δ^{18}O does not reach its glacial maximum until immediately before each termination, due to continuing ice sheet growth [*Thompson and Goldstein*, 2006; *Lea et al.*, 2002]. Glacial trends in $\Delta\delta^{13}C_{P-\frac{NA}{2}}$ match those of pCO_2, with $\Delta\delta^{13}C_{P-\frac{NA}{2}}$ reaching a minimum 30–40 kyr before the δ^{18}O maximum during most glaciations (Figure 2, bottom). Additionally, $\Delta\delta^{13}C_{P-\frac{NA}{2}}$ correlates better with the magnitudes of glacial pCO_2 minima than δ^{18}O does. In $\Delta\delta^{13}C_{P-\frac{NA}{2}}$ and pCO_2, MIS 12 is less extreme than MIS 8, 10, and 16, whereas in δ^{18}O MIS 12 is similar to MIS 16 and more extreme than MIS 8 and 10. Thus, $\Delta\delta^{13}C_{P-\frac{NA}{2}}$ reproduces

Table 1. Proxy Correlation With pCO_2 for 800–0 ka

Proxy	Correlation
N. Atlantic δ^{13}C[a]	0.19
Deep S. Atl δ^{13}C[a]	0.69
Deep Pacific δ^{13}C[a]	0.66
$\Delta\delta^{13}C_{P-NA}$[a]	0.58
$\Delta\delta^{13}C_{P-\frac{NA}{2}}$[a]	0.75
log(alkenone conc.)[b]	−0.71
Tropical SST stack[c]	0.64

[a]See auxiliary material for component records.
[b]Site ODP 1090 [*Martínez-Garcia et al.*, 2009] (see auxiliary material for age model).
[c]*Herbert et al.* [2010].

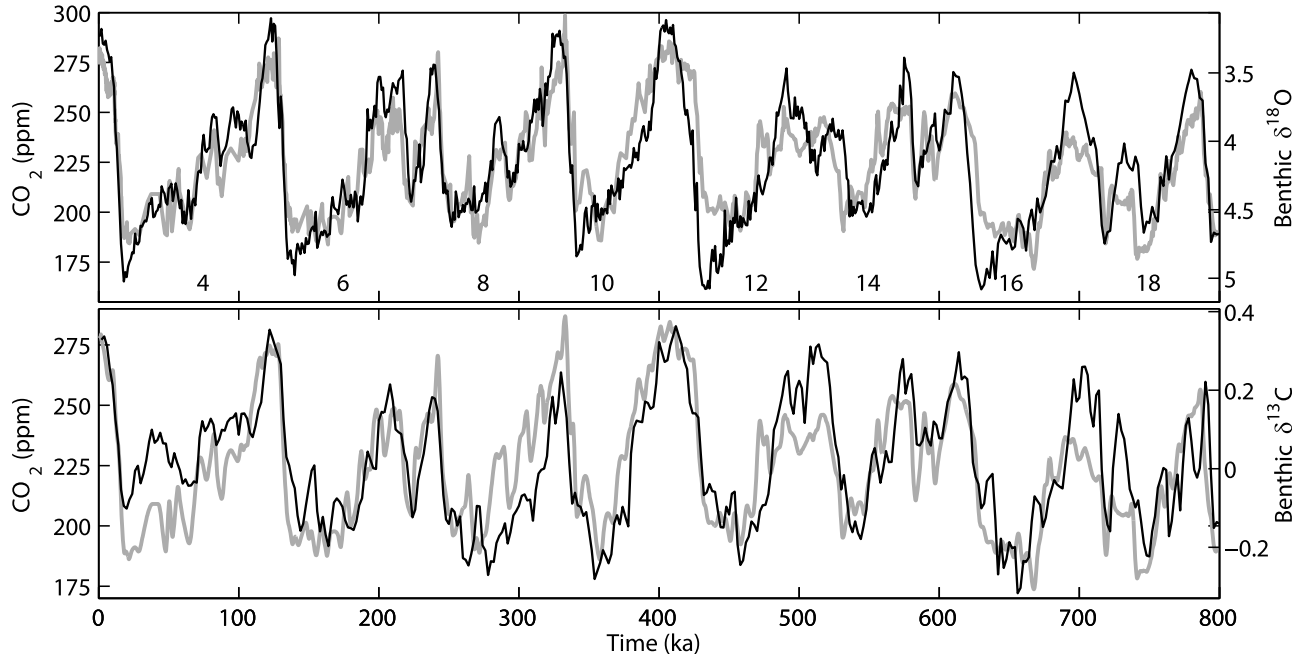

Figure 2. Comparison of pCO_2 (gray) [*Petit et al.*, 1999; *Monnin et al.*, 2001; *Siegenthaler et al.*, 2005; *Lüthi et al.*, 2008] with (top) benthic $\delta^{18}O$ (black) [*Lisiecki and Raymo*, 2005] and (bottom) $\Delta\delta^{13}C_{P-\frac{N4}{2}}$ (black). Glacial stages are labeled by MIS number. In Figure 2 (bottom), pCO_2 has been smoothed with a 2-kyr boxcar filter.

many pCO_2 responses that are independent of age model uncertainty and differ from ice volume change.

4. Termination Lags Between pCO_2 and $\delta^{18}O$

[11] Comparison of $\Delta\delta^{13}C_{P-\frac{N4}{2}}$ and the ice core pCO_2 record provides an opportunity to link marine and ice core age models. Abrupt increases in pCO_2 and $\Delta\delta^{13}C_{P-\frac{N4}{2}}$ have similar ages on their respective age models (Table S2), suggesting that the marine and ice core age models [*Lisiecki and Raymo*, 2005; *Parrenin et al.*, 2007; *Loulergue et al.*, 2007] are consistent to within 2.7 kyr during terminations. However, age model evaluation away from terminations is hampered by weaker correlation of the records' suborbital-scale variability.

[12] Climatic lags between pCO_2 and ice volume during terminations are evaluated by comparing $\Delta\delta^{13}C_{P-\frac{N4}{2}}$ and benthic $\delta^{18}O$ changes within marine sediments. During most terminations $\Delta\delta^{13}C_{P-\frac{N4}{2}}$ leads $\delta^{18}O$ by 0.2–3.7 kyr, but $\Delta\delta^{13}C_{P-\frac{N4}{2}}$ lags $\delta^{18}O$ by 9.8 and 3.5 kyr during Termination 6 (535 ka) and MIS 18 (745 ka), respectively (Table S3). These lags are also found between benthic $\delta^{18}O$ and $\delta^{13}C$ within individual Pacific cores (Figure S2). An anomalous phase relationship between ice volume and pCO_2 may explain why these two warming events are weaker than most Late Pleistocene terminations. During both "failed" terminations, the initial $\delta^{18}O$ change is approximately half the amplitude of most Late Pleistocene terminations; $\delta^{18}O$ spends ~20 kyr at intermediate values of 3.8–4.2‰ and then briefly returns to more glacial values before achieving full interglacial conditions ~40 kyr after the initial warming. The $\Delta\delta^{13}C_{P-\frac{N4}{2}}$ lag during these two failed terminations suggests that full deglaciation requires an early pCO_2 response.

[13] The initial trigger for terminations and the mechanistic link between pCO_2 and northern hemisphere ice volume remain controversial [e.g., *Huybers*, 2009; *Denton et al.*, 2010]. Variability in the phase between $\delta^{18}O$ and $\Delta\delta^{13}C_{P-\frac{N4}{2}}$ supports the hypothesis of *Toggweiler* [2008] that glacial changes in pCO_2 are controlled by southern hemisphere processes only weakly linked to northern hemisphere insolation and ice volume. However, tighter coupling between the hemispheres appears to develop at ~500 ka, as suggested by smaller phase differences between $\Delta\delta^{13}C_{P-\frac{N4}{2}}$ and $\delta^{18}O$ (Table S3), an increase in pCO_2 amplitude, and the phase lock between Antarctic temperature and northern hemisphere insolation during the last five terminations [*Kawamura et al.*, 2007].

5. Estimates of pCO_2 for 1.5–0.8 Ma

[14] Here $\Delta\delta^{13}C_{P-\frac{N4}{2}}$-based estimates of pCO_2 from 1.5–0.8 Ma are compared with several other paleoclimate records that may correlate with pCO_2. A proxy for South Atlantic surface productivity (the logarithm of alkenone concentration at ODP Site 1090) [*Martínez-Garcia et al.*, 2009] reproduces of the same glacial trends observed in pCO_2 and $\Delta\delta^{13}C_{P-\frac{N4}{2}}$ (Figure 3, top) and has a similar correlation with pCO_2 (Table 1). Although South Atlantic productivity change appears to explain only 40–50 ppm of Late Pleistocene pCO_2 fluctuation, the proxy's correlation with pCO_2 may be enhanced by sensitivity to climate changes correlated with pCO_2, such as South American aridity and westerly wind strength [*Martínez-Garcia et al.*, 2009]. Similarity between $\Delta\delta^{13}C_{P-\frac{N4}{2}}$ and the alkenone record from 1.1–0.8 Ma provides additional support for the reliability of both proxies, particularly because they are linked to pCO_2 by different mechanisms.

[15] Both empirical proxies indicate that pCO_2 generally varies between 180–260 ppm from 1.1–0.8 Ma, except for a large oscillation at 950–900 ka (Figure 3, top). Both suggest a pCO_2 minimum at 920 ka of ~155 ppm, i.e., less than the

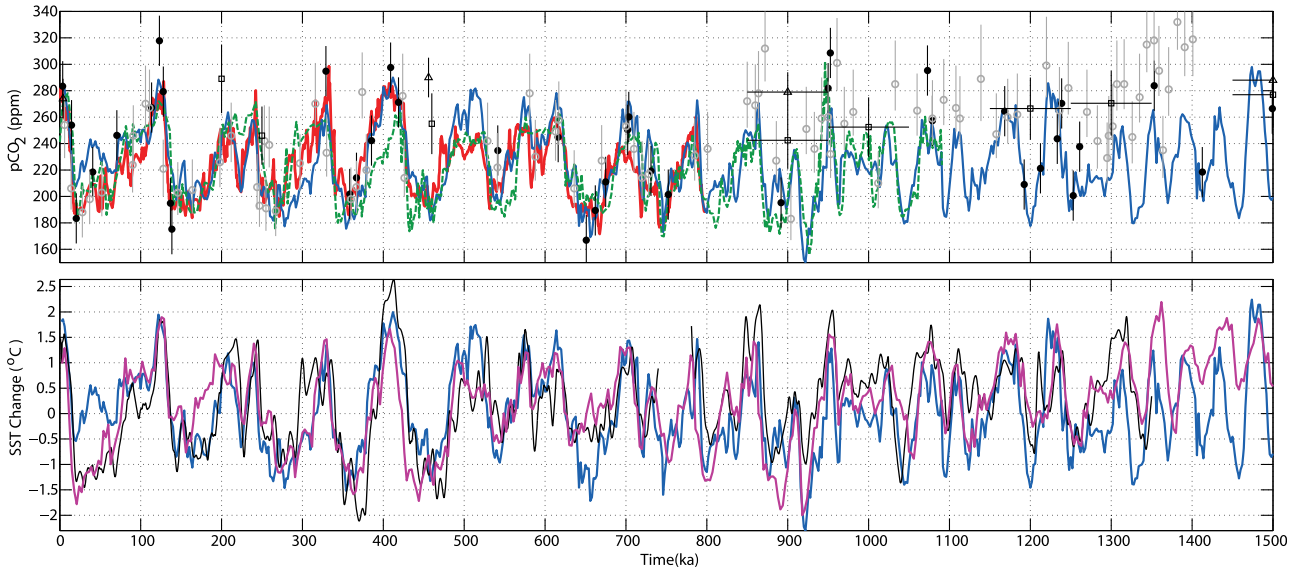

Figure 3. Proxy comparison. (top) pCO_2 (red) [*Petit et al.*, 1999; *Monnin et al.*, 2001; *Siegenthaler et al.*, 2005; *Lüthi et al.*, 2008], $\Delta\delta^{13}C_{P-\frac{NA}{2}}$ (blue), alkenone concentration (green dashed) [*Martínez-Garcia et al.*, 2009], boron-based estimates with error bars (black dots [*Hönisch et al.*, 2009]; gray circles [*Tripati et al.*, 2009]; triangles [*Seki et al.*, 2010]), and alkenone $\delta^{13}C$ estimates (squares) [*Seki et al.*, 2010]. $\Delta\delta^{13}C_{P-\frac{NA}{2}}$ and alkenone proxies are scaled to ppm using the mean and standard deviation of pCO_2 from 800–0 ka. (See auxiliary material for ODP 1090 age model.) (bottom) Changes in $\Delta\delta^{13}C_{P-\frac{NA}{2}}$ (blue), WEP SST [*Medina-Elizalde and Lea*, 2005], and a tropical SST stack (purple) [*Herbert et al.*, 2010] with trend reduced by 0.29°C/Myr to match the WEP. $\Delta\delta^{13}C_{P-\frac{NA}{2}}$ is scaled to °C using the standard deviation of the SST stack from 500–100 ka.

ice core pCO_2 minimum of 172 ppm at 668 ka. Many other paleoclimate records also contain evidence for extreme climatic conditions at ~900 ka, including anomalously low sea surface temperatures (SST), ocean circulation change, and increased Asian aridity [*Clark et al.*, 2006].

[16] The increase in glacial benthic $\delta^{18}O$ values across the mid-Pleistocene transition (MPT) from 1.3–0.6 Ma is often attributed to decreasing glacial pCO_2 values [e.g., *Raymo*, 1997; *Herbert et al.*, 2010]. Although $\Delta\delta^{13}C_{P-\frac{NA}{2}}$ gradually shifts from 41-kyr to 100-kyr cyclicity from 1.3–0.7 Ma (Figure S3), it does not match the secular trend or amplitude increase observed in benthic $\delta^{18}O$ from 1.3–0.6 Ma. Boron-based measurements suggest that glacial pCO_2 minima decrease at ~800 ka [*Hönisch et al.*, 2009; *Tripati et al.*, 2009], but these sparse measurements may not reliably sample glacial minima (Figure 3, top). The $\Delta\delta^{13}C_{P-\frac{NA}{2}}$ and alkenone proxies, which show no change in glacial pCO_2 minima, actually agree with the low-resolution pCO_2 estimates of *Hönisch et al.* [2009] and *Seki et al.* [2010] from 1.5–0.8 Ma to within uncertainty (including age uncertainty). Also, the results of a carbon cycle box model suggest that a change in glacial pCO_2 minima during the MPT cannot be reconciled with the amplitude of Pacific $\delta^{13}C$ variability [*Köhler and Bintanja*, 2008].

[17] Additionally, SST change at some tropical sites unaffected by upwelling is thought to be driven by changes in radiative forcing [*Medina-Elizalde and Lea*, 2005; *Herbert et al.*, 2010]. An SST record from the Western Equatorial Pacific (WEP) warm pool shows no significant trend from 1.35–0.5 Ma [*Medina-Elizalde and Lea*, 2005], consistent with the results of the $\Delta\delta^{13}C_{P-\frac{NA}{2}}$ and alkenone proxies. A recent tropical SST stack that includes both upwelling and non-upwelling sites shows a slight cooling trend [*Herbert et al.*, 2010], but if its long-term trend is adjusted to match the SST trend of the WEP and other non-upwelling sites, the SST stack agrees well with $\Delta\delta^{13}C_{P-\frac{NA}{2}}$ from 1.25–0.2 Ma (Figure 3 (bottom) and auxiliary material). Thus, only the pCO_2 estimates of *Tripati et al.* [2009] are inconsistent with steady glacial pCO_2 minima since 1.25 Ma.

[18] However, before 1.25 Ma glacial temperatures in the trend-adjusted stack are ≥1°C warmer than would be expected based on $\Delta\delta^{13}C_{P-\frac{NA}{2}}$. The SST stack could be affected by possible upwelling change at 1.25 Ma, such as thermocline shoaling or cooling at source water formation sites. However, a change in the relationship between $\Delta\delta^{13}C_{P-\frac{NA}{2}}$ and pCO_2 is also possible, perhaps as the result of circulation or whole-ocean ΣCO_2 change. Additional high-resolution proxies are needed to improve confidence in glacial pCO_2 estimates, especially before 1.25 Ma.

6. Conclusions

[19] In conclusion, $\Delta\delta^{13}C_{P-\frac{NA}{2}}$ correlates well with ice core pCO_2 from 800–0 ka and reproduces many features of the pCO_2 record. Comparison of $\Delta\delta^{13}C_{P-\frac{NA}{2}}$ and pCO_2 suggests that marine and ice core age models [*Lisiecki and Raymo*, 2005; *Parrenin et al.*, 2007; *Loulergue et al.*, 2007] differ by ≤2.7 kyr at terminations. Within the marine sedimentary record $\Delta\delta^{13}C_{P-\frac{NA}{2}}$ usually leads $\delta^{18}O$ by 0.2–3.7 kyr at terminations but lags by 3–10 kyr during "failed" terminations at 535 and 745 ka. Thus, an early pCO_2 response appears necessary for complete deglaciation, and pCO_2 appears less tightly coupled to northern hemisphere ice volume before 500 ka.

[20] Several proxies that correlate with pCO_2 ($\Delta\delta^{13}C_{P-\frac{NA}{2}}$, South Atlantic productivity [*Martínez-Garcia et al.*, 2009], and WEP SST [*Medina-Elizalde and Lea*, 2005]) and a carbon cycle box model [*Köhler and Bintanja*, 2008] suggest

that glacial pCO_2 minima do not decrease during the MPT. Moreover, the minimum pCO_2 concentration of the last 1.5 Myr is estimated to occur at 920 ka. $\Delta\delta^{13}C_{P-\frac{N4}{2}}$ gradually shifts from 41-kyr cycles to 100-kyr cycles from 1.3–0.7 Ma but shows no secular trend in mean or amplitude over the last 1.5 Myr, whereas tropical SST records suggest warmer glacial maxima before 1.3 Ma [*Herbert et al.*, 2010]. This likely indicates that at least one of these proxies is affected by factors other than pCO_2 before 1.3 Ma; thus, additional high-resolution proxies are needed.

[21] **Acknowledgments.** I thank D. Lea, D. Raynaud, T. Herbert, M. Raymo and two anonymous reviewers for useful suggestions and discussions. Support provided by NSF-MGG 0926735.

References

Brovkin, V., A. Ganopolski, D. Archer, and S. Rahmstorf (2007), Lowering of glacial atmospheric CO_2 in response to changes in oceanic circulation and marine biogeochemistry, *Paleoceanography*, *22*, PA4202, doi:10.1029/2006PA001380.

Clark, P. U., D. Archer, D. Pollard, J. D. Blum, J. A. Rial, V. Brovkin, A. C. Mix, N. G. Pisias, and M. Roy (2006), The middle Pleistocene transition: Characteristics, mechanisms, and implications for long-term changes in atmospheric pCO_2, *Quat. Sci. Rev.*, *25*, 3150–3184.

Denton, G. H., R. F. Anderson, J. R. Toggweiler, R. L. Edwards, J. M. Schaefer, and A. E. Putnam (2010), The last glacial termination, *Science*, *328*, 1652–1656.

Flower, B. P., D. W. Oppo, J. F. McManus, K. A. Venz, D. A. Hodell, and J. L. Cullen (2000), North Atlantic Intermediate to Deep Water circulation and chemical stratification during the past 1 Myr, *Paleoceanography*, *15*, 388–403.

Hansen, J., M. Sato, P. Kharecha, G. Russell, D. W. Lea, and M. Siddall (2007), Climate change and trace gases, *Philos. Trans. R. Soc. A*, *365*, 1925–1954.

Herbert, T. D., L. Cleaveland Peterson, K. T. Lawrence, and Z. Liu (2010), Tropical ocean temperatures over the past 3.5 million years, *Science*, *328*, 1530–1534.

Hodell, D. A., K. A. Venz, C. D. Charles, and U. S. Ninnemann (2003), Pleistocene vertical carbon isotope and carbonate gradients in the South Atlantic sector of the Southern Ocean, *Geochem. Geophys. Geosyst.*, *4*(1), 1004, doi:10.1029/2002GC000367.

Hönisch, B., N. G. Hemming, D. Archer, M. Siddall, and J. F. McManus (2009), Atmospheric carbon dioxide concentration across the mid-Pleistocene transition, *Science*, *324*, 1551–1553.

Huybers, P. (2009), Antarctica's orbital beat, *Science*, *325*, 1085–1086.

Jouzel, J., et al. (2007), Orbital and millennial Antarctic climate variability over the last 800,000 years, *Science*, *317*, 793–796.

Kawamura, K., et al. (2007), Northern Hemisphere forcing of climatic cycles in Antarctica over the past 360,000 years, *Nature*, *448*, 912–917.

Köhler, P., and R. Bintanja (2008), The carbon cycle during the Mid Pleistocene Transition: The Southern Ocean decoupling hypothesis, *Clim. Past*, *4*, 311–332.

Köhler, P., H. Fischer, and J. Schmitt (2010), Atmospheric $\delta^{13}CO_2$ and its relation to pCO_2 and deep ocean δ^{13} during the late Pleistocene, *Paleoceanography*, *25*, PA1213, doi:10.1029/2008PA001703.

Lea, D. W. (2004), The 100,000-yr cycle in tropical SST, greenhouse forcing, and climate sensitivity, *J. Clim.*, *17*, 2170–2179.

Lea, D. W., P. A. Martin, D. K. Pak, and H. J. Spero (2002), Reconstructing a 350 ky history of sea level using planktonic Mg/Ca and oxygen isotope records from a Cocos Ridge core, *Quat. Sci. Rev.*, *21*, 283–293.

Lisiecki, L. E. (2010), A simple mixing explanation for late Pleistocene changes in the Pacific-South Atlantic benthic δ^{13}C gradient, *Clim. Past*, *6*, 305–314.

Lisiecki, L. E., and M. E. Raymo (2005), A Pliocene-Pleistocene stack of 57 globally distributed benthic δ^{18}O records, *Paleoceanography*, *20*, PA1003, doi:10.1029/2004PA001071.

Loulergue, L., F. Parrenin, T. Blunier, J.-M. Barnola, R. Spahni, A. Schilt, G. Raisbeck, and J. Chappellaz (2007), New constraints on the gas age-ice age difference along the EPICA ice cores, 0–50 kyr, *Clim. Past*, *3*, 527–540.

Lüthi, D., et al. (2008), High-resolution carbon dioxide concentration record 650,000–800,000 years before present, *Nature*, *453*, 379–382.

Martínez-Garcia, A., A. Rosell-Melé, W. Geibert, R. Gersonde, P. Masqué, V. Gaspari, and C. Barbante (2009), Links between iron supply, marine productivity, sea surface temperature, and CO2 over the last 1.1 Ma, *Paleoceanography*, *24*, PA1207, doi:10.1029/2008PA001657.

Matsumoto, K., T. Oba, J. Lynch-Stieglitz, and H. Yamamoto (2002), Interior hydrography and circulation of the glacial Pacific Ocean, *Quat. Sci. Rev.*, *21*, 1693–1704.

Medina-Elizalde, M., and D. W. Lea (2005), The mid-Pleistocene transition in the tropical Pacific, *Science*, *310*, 1009–1012.

Monnin, E., A. Indermühle, A. Dällenbach, J. Flückiger, B. Stauffer, T. F. Stocker, D. Raynaud, and J.-M. Barnola (2001), Atmospheric CO_2 concentrations over the last glacial termination, *Science*, *291*, 112–114.

Oppo, D. W., and R. G. Fairbanks (1990), Atlantic Ocean thermohaline circulation of the last 150,000 years: Relationship to climate and atmospheric CO_2, *Paleoceanography*, *5*, 277–288.

Pagani, M., Z. Liu, J. LaRiviere, and A. C. Ravelo (2009), High Earth-system climate sensitivity determined from Pliocene carbon dioxide concentrations, *Nat. Geosci.*, *3*, 27–30.

Parrenin, F., et al. (2007), The EDC3 chronology for the EPICA Dome C ice core, *Clim. Past*, *3*, 485–497.

Petit, J. R., et al. (1999), Climate and atmospheric history of the past 420,000 years from the Vostok ice core, Antarctica, *Nature*, *399*, 429–436.

Raymo, M. E. (1997), The timing of major climate terminations, *Paleoceanography*, *12*, 577–585.

Seki, O., G. L. Foster, D. N. Schmidt, A. Mackensen, K. Kawamura, and R. D. Pancost (2010), Alkenone and boron-based Pliocene pCO_2 records, *Earth Planet. Sci. Lett.*, *292*, 201–211.

Shackleton, N. J. (1977), Carbon-13 in Uvigerina: Tropical rainforest history and the equatorial Pacific carbonate dissolution cycles, in *The Fate of Fossil Fuel CO_2 in the Oceans*, edited by N. R. Andersen and A. Malahoff, pp. 401–428, Plenum, New York.

Siegenthaler, U., et al. (2005), Stable carbon cycle-climate relationship during the late Pleistocene, *Science*, *310*, 1313–1317.

Thompson, W. G., and S. L. Goldstein (2006), A radiometric calibration of the SPECMAP timescale, *Quat. Sci. Rev.*, *25*, 3207–3215.

Toggweiler, J. R. (1999), Variation of atmospheric CO_2 by ventilation of the ocean's deepest water, *Paleoceanography*, *14*, 571–588.

Toggweiler, J. R. (2008), Origin of the 100,000-year timescale in Antarctic temperatures and atmospheric CO_2, *Paleoceanography*, *23*, PA2211, doi:10.1029/2006PA001405.

Toggweiler, J. R., J. L. Russell, and S. R. Carson (2006), Midlatitude westerlies, atmospheric CO_2, and climate change during the ice ages, *Paleoceanography*, *21*, PA2005, doi:10.1029/2005PA001154.

Tripati, A. R., C. D. Roberts, and R. A. Eagle (2009), Coupling of CO_2 and ice sheet stability over major climate transitions of the last 20 million years, *Science*, *326*, 1394–1397.

Venz, K. A., and D. A. Hodell (2002), New evidence for changes in Plio-Pleistocene deep water circulation from Southern Ocean ODP Leg 177 Site 1090, *Palaeogeogr. Palaeoclimatol. Palaeoecol.*, *182*, 197–220.

L. E. Lisiecki, Department of Earth Science, University of California, Santa Barbara, CA 93106, USA. (lisiecki@geol.ucsb.edu)